AJNR

Healing Response in Elastase-Induced Rabbit Aneurysms after Embolization with a New Platinum Coil System

Naomi H. Fujiwara and David F. Kallmes

AJNR Am J Neuroradiol 2002, 23 (7) 1137-1144
http://www.ajnr.org/content/23/7/1137

AJNR Am J Neuroradiol 23:1137–1144, August 2002

Healing Response in Elastase-Induced Rabbit Aneurysms after Embolization with a New Platinum Coil System

Naomi H. Fujiwara and David F. Kallmes

BACKGROUND AND PURPOSE: **Elastase-induced rabbit aneurysms offer promise in preclinical testing, but their radiographic and histologic features after dense packing with platinum coils are unknown. We evaluated these features by using a new platinum coil system.**

METHODS: **Right common carotid arterial (CCA) aneurysms were created in 17 rabbits by distal ligation and intraluminal elastase incubation. At least 3 weeks later, aneurysms were packed with detachable platinum coils. Animals were sacrificed at 2 (group 1, n = 4), 4 (group 2, n = 5), 12 (group 3, n = 4), or 24 (group 4, n = 4) weeks. Aneurysmal occlusion and coil compaction were angiographically assessed. Histologic features of tissue covering the coils and the aneurysmal dome were assessed and semiquantitatively compared across groups.**

RESULTS: **No notable tracking, deployment, or detachment problems occurred. Volumetric occlusion was 5–49% (mean, 26.8% ± 11%). Angiographic occlusion was 100% in six cases, 95% in four, and 90% in seven; occlusion scores remained unchanged in 13 cases, decreased in one, and increased in two (one case excluded from angiographic follow-up). Histologic findings were concordant within groups. Group 1 had coverage with thin fibrin layers and scattered leukocytes; group 2, some spindle-cell coverage; group 3, spindle-cell coverage. In groups 1 and 2, dome findings included only unorganized blood products. In group 3, blood products had been replaced with a hypocellular, poorly staining matrix. Some group 4 subjects had variably aged blood products, with tissue of limited organization.**

CONCLUSION: **The platinum coil system performed well in experimental aneurysmal embolization. Densely packed rabbit aneurysms demonstrate reproducible histologic evolution: early fibrin coverage, delayed spindle-cell coverage, delayed intraaneurysmal thrombus resorption, and occasional coil compaction.**

Preclinical assessment of emerging aneurysm therapies is greatly facilitated by reproducible experimental models. Numerous animal models have been proposed as valid systems: for example, the rat, rabbit, canine, swine, sheep, and primate models (1–13). Both arterial and vein-pouch aneurysms have been suggested. Recently, an elastase-induced aneurysm model in rabbits has been proposed for testing coil modifications (1, 7, 14). This technique involves the ligation of the common carotid artery (CCA) and elastase treatment of the vessel wall. The size and shape of the resultant aneurysmal cavities simulate those of human intracranial aneurysms, and the tortuosity and diameter of the parent artery model those of human intracranial vessels.

Although the elastase-induced rabbit model offers promise as a preclinical testing device, data regarding radiographic findings and histologic evolution after dense packing with platinum coils is lacking. In the current study, our purpose was to assess the angiographic and histologic findings in an elastase-induced aneurysm model after embolization by using a new, detachable platinum coil system.

Methods

Subjects

Seventeen New Zealand white rabbits (3–4 kg) were used in this study. The duration of coil implantation was 2 weeks in four subjects, 4 weeks in five subjects, 12 weeks in four subjects, and 24 weeks in four subjects. The 4-week group had one extra subject, because we had embolized an aneurysm in one addi-

Received December 3, 2001; accepted after revision April 1, 2002.

Supported by Microvention, Inc., Aliso Viejo, CA.

Presented at the 40th annual meeting of the American Society of Neuroradiology, May 2002, Vancouver, B.C., Canada.

From the Department of Radiology, University of Virginia Health Services, Charlottesville.

Address reprint requests to David F. Kallmes, MD, Box 170, Department of Radiology, University of Virginia Health Services, Charlottesville, VA 22908.

tional rabbit to serve as an alternate in case of unanticipated morbidity or mortality in the long-term groups. Because no unexpected morbidity or mortality occurred, the extra subject was sacrificed at 4 weeks to diminish per diem costs, and this subject was included in the 4-week group.

Device Construction

The MicroPlex coil system (MicroVention, Inc, Aliso Viejo, CA) comprises complex coils and filler platinum coils in 0.010-inch and 0.018-inch sizes. The complex coils have a unique multiaxis configuration and were deployed first in the aneurysm to establish a cagelike framework. Filler coils have a helical configuration after basket formation is achieved. Complex and filler coils with a variety of diameters (2–8 mm) and lengths (4–20 cm) were evaluated in this study.

The coils were detached from the pusher by using a fluid-actuated detachment system. Manual pressure was applied to the proximal end of the pusher tube by using a 1-mL syringe filled with radiographic contrast medium (Omnipaque 300; Nycomed, Princeton, NJ). The pressure was transmitted through the lumen of the pusher tube to its distal tip. The pressure actuated the detachment of the coil from the pusher, resulting in instantaneous detachment.

Aneurysm Creation

Detailed procedures for aneurysm creation are described elsewhere (15). Briefly, New Zealand white rabbits (3–4 kg) were anesthetized with ketamine and xylazine (60 and 6 mg/kg, respectively). By using sterile technique, the right CCA was exposed and distally ligated. A 5F sheath (Cordis Endovascular, Miami Lakes, FL) was advanced in a retrograde fashion in the CCA to a point approximately 3 cm cephalic to the CCA origin. Through this indwelling sheath, a 3F Fogarty balloon (Baxter Healthcare Corp, Irvine, CA) was advanced to the origin of the right CCA at its junction with the subclavian artery. The balloon was inflated with iodinated contrast material (Omnipaque), just enough to arrest flow in the CCA. Porcine elastase (5.23 U/mg P, 40.1 mg P/mL, approximately 200 U/mL; Worthington Biochemical Corp, Lakewood, NJ) mixed with saline and iodinated contrast material (Omnipaque) was incubated in the dead space of the CCA above the inflated balloon. After incubation of the elastase solution, the balloon and sheath were removed, and the CCA was ligated below the sheath entry site.

Coil Embolization

Aneurysms were allowed to mature for at least 3 weeks after their creation. For the embolization procedure, anesthesia was induced with an intramuscular injection of ketamine and xylazine; this was followed by maintenance anesthesia with intravenously administered pentobarbital. By using sterile technique, the right common femoral artery (CFA) was surgically exposed. The distal part of the artery was ligated by using 4–0 silk sutures, and a 22-gauge angiocatheter was advanced in retrograde fashion into the artery. An 0.018-inch guidewire was passed through the angiocatheter; this step was followed by the placement of a 5F vascular sheath. Heparin (100 U/kg) was administered intravenously. A 5F catheter (Envoy, Cordis Neurovascular Systems, Miami Lakes, FL) was advanced into the brachiocephalic artery. By using a coaxial technique, with a continuous heparin and saline flush, a two-marker microcatheter (Rapid Transit; Cordis Neurovascular or Excel; Target Therapeutics) was advanced into the aneurysmal cavity. The size of the aneurysmal cavity was assessed by directly comparing it with radiopaque sizing devices. In all cases, one or more complex coils were initially placed, followed by subsequent packing with filler coils. Coils were detached by using a fluid-actuated mechanism. Aneurysms were packed as densely as possible. After embolization, final control digital subtraction angiography (DSA) was performed. An experienced observer (D.F.K.) estimated the percentage of aneurysm occlusion by using the following categories: 100% occluded, 95% occluded, 90% occluded, or less than 90% occluded. Percentage of volumetric occlusion was also calculated. The sheath and catheters were removed, the femoral artery ligated, and the skin closed with running sutures.

Follow-up Imaging and Tissue Harvesting

Animals were followed up and sacrificed at various intervals after coil embolization: 2 weeks (group 1, n = 4), 4 weeks (group 2, n = 5), 12 weeks (group 3, n = 4), and 24 weeks (group 4, n = 4). Subjects sacrificed at 2 or 4 weeks underwent intraarterial DSA at the time of sacrifice. Subjects followed up for 12 weeks underwent intravenous DSA at 8 weeks and intraarterial DSA at the time of sacrifice. Subjects followed up for 24 weeks underwent intravenous DSA at 16 weeks and intraarterial DSA at the time of sacrifice. All follow-up angiograms were compared with the angiograms obtained immediately after embolization to assess interval changes in coil configuration and aneurysmal filling.

On the day of sacrifice, the left CFA was surgically accessed, in a fashion similar to that used to access the right CFA, as described earlier. A 4F catheter was placed in the aortic arch, and DSA was performed. Immediately after angiography, subjects were euthanized by use of lethal-injection pentobarbital. Saline, followed by formalin, was rapidly injected through the indwelling catheter. The mediastinum was dissected, and the aortic arch and proximal great vessels, including the coil-embolized segment of artery, were exposed and dissected free from surrounding tissues. The tissue was immediately placed in formalin. Tissue was embedded in methylmethacrylate, sectioned, and stained with hematoxylin and eosin. An experienced pathologist viewed the sections, paying particular attention to the cell type and the appearance of the extracellular matrix within and around the coil mass.

Histologic Evaluation

Qualitative and semiquantitative evaluations were performed in the aneurysmal neck, which was defined as the interface between the parent artery and the aneurysmal cavity, and in the aneurysmal dome. In the aneurysmal neck, the tissue type, thickness, and cellularity were graded by using a three-point scale. Grade 0 was a thin layer of fibrin with scattered polymorphonuclear leukocytes; grade 1, a thick layer of fibrin with scattered polymorphonuclear leukocytes; and grade 2, a thin layer of spindle cells. The thickness of tissue covering the coils at the aneurysmal neck was calculated on the basis of the thinnest visible covering at any one point along the neck. The shape of the tissue at the coil–parent artery interface was described as convex, flat, or concave. The tissue within the dome of the aneurysm was qualitatively described by using a four-point scale. Grade 0 was only unorganized blood; grade 1, mostly unorganized blood; grade 2, small amount of unorganized blood; and grade 3, a hypocellular matrix without blood products.

Results

Aneurysmal Size

Mean aneurysmal width was 4.7 mm ± 1.3 (range, 3.2–7.7 mm). Mean aneurysmal height was 8.6 mm ± 2.6 (range, 4.1–13 mm). Mean neck width was 4.4 mm ± 1.3 (range, 3–8 mm). The mean dome-to-neck ratio was 1.1 ± 0.2 (range, 0.7–1.7). All aneurysms were successfully embolized.

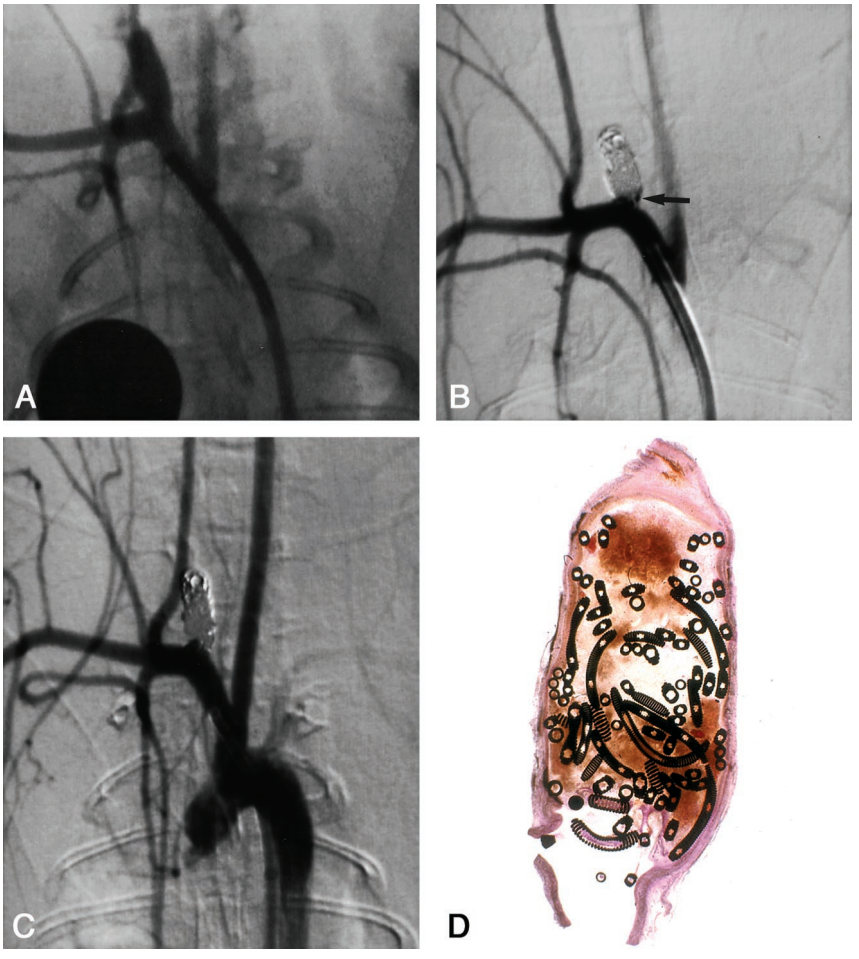

FIG 1. Subject 3, 2-week implantation.
A, DSA image obtained before embolization. Aneurysm measures 3.8 × 3 × 10 mm (width × neck × length).
B, DSA image obtained immediately after embolization shows 95% occlusion and a tiny triangular neck remnant (*arrow*).
C, Angiogram obtained before animal was sacrificed and 2 weeks after coil embolization shows complete occlusion.
D, Photomicrograph reveals unorganized blood filling the aneurysmal cavity. The neck of the aneurysm is covered with a thin, fibrin rim (hematoxylin-eosin stain, original magnification ×6.3).

Device Performance

In all cases, the first coil placed was a complex coil. In 10 of 17 aneurysms, only one complex coil was placed. In the remaining seven aneurysms, two to five complex coils were placed. A total of 34 complex coils and 60 filler coils were deployed. All 34 complex coils deployed and achieved a cagelike framework in the wide-necked aneurysms. All 60 filler coils were placed inside the complex coil basket. Coils were readily detached in 90 (96%) of 94 deployments. Detachment failures were related to production errors in four coils. Percentage of volumetric occlusion was 5–49% (mean, 26.8% ± 11%).

Angiographic Evaluation and Follow-up

Immediately after embolization, angiographic occlusion scores were 100% in six (35%) of 17 cases, 95% in four (24%), and 90% in seven (41%). Angiographic occlusion scores remained unchanged throughout the follow-up period in 13 (81%) of 16 cases, decreased in one (6%), and increased in two (12%). One case was excluded from angiographic follow-up analysis, because histologic analysis later showed that the coils had been inadvertently placed into a dissection flap rather than the aneurysmal cavity (see 24-week results in Histologic Evaluation). In four (23%) cases, single loops of coil protruded into the parent artery, without evidence of parent artery compromise either immediately after embolization or at follow-up. Angiograms are shown in Figures 1–5.

Histologic Evaluation

Among subjects sacrificed 2 weeks after coil implantation, aneurysmal domes were filled with unorganized thrombus in all four cases (mean dome histologic score, 0). Fibrin and scattered inflammatory cells were present at the neck in all four cases (mean neck histologic score, 0.5; range 0–1) (Fig 1D).

Among subjects sacrificed 4 weeks after coil implantation, aneurysmal domes were completely filled with unorganized thrombus in one case, predominantly filled with unorganized thrombus in three cases, and devoid of unorganized thrombus in one case (mean dome histologic score, 1.2; range 0–3). Two cases had fibrin and inflammatory cells across the neck, whereas three cases had a thin layer of spindle cells across the neck (mean neck histologic score, 1.6; range 1–2) (Fig 2D).

Among subjects sacrificed 12 weeks after coil implantation, unorganized thrombus was completely absent in the aneurysmal dome in three cases, and a small amount of residual unorganized thrombus was present in one case (mean dome histologic score, 2.8; range, 2–3). A thin layer of spindle cells covered the

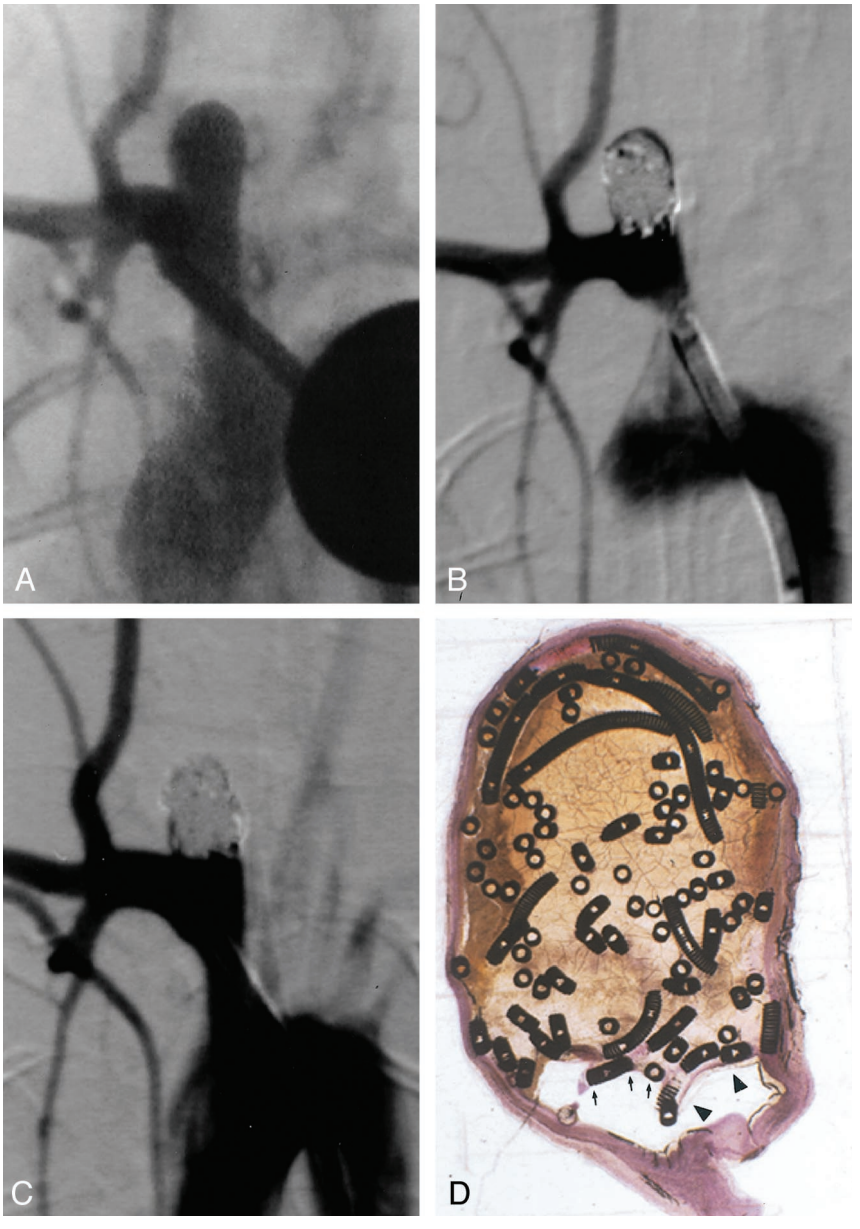

FIG 2. Subject 7, 4-week implantation.
A, DSA obtained image before embolization. The aneurysm is 4.9 × 5.1 × 6.5 mm (width × neck size × length).
B, DSA image obtained immediately after embolization depicts 95% occlusion.
C, Angiogram obtained before euthanasia and 4 weeks after coil implantation shows no change.
D, Photomicrograph reveals mostly unorganized blood filling the aneurysmal cavity and a thin fibrin rim covering the coils (*arrows*) (hematoxylin-eosin stain, original magnification ×6.3). The neck of the aneurysm is covered with thin fibrin rim (*arrowheads*).

neck in all four cases (mean neck histologic score, 2.0) (Fig 3D).

Among subjects sacrificed 24 weeks after coil implantation, two of four cases had aneurysmal domes that were completely devoid of unorganized thrombus. Both of these cases had spindle cells across the aneurysmal necks. One of four cases showed marked recanalization of the dome, with laminated blood products of various ages. The neck of this aneurysm was covered with only fibrin. In one of four cases, the embolized portion of the artery was a dissection cavity separate from the aneurysm itself, and this aneurysm was excluded from analysis (Figs 4D and 5D).

In all cases at all time points, at least some of the coils in immediate contact with the parent artery was essentially bare, with no demonstrable tissue overgrowth.

The morphology of the tissue-blood interface at the aneurysmal neck was flat in six (38%) of 16 cases, concave in nine (56%), and convex in one (6%). Discerning whether a concave parent artery–aneurysmal neck interface represented microcompaction or simply the morphology of the coils as initially placed during embolization was not possible.

Discussion

This study was a detailed analysis of the healing response of elastase-induced aneurysms in rabbits after they were densely packed with a new platinum coil system. The angiographic findings in our study demonstrated a stable coil configuration in most of the cases, with slight compaction seen in 6% of the aneurysms. This finding concurs with those of a clinical series (16) that had similar rates of compaction among aneurysms with a diameter less than 10 mm, such as those used in our study. The histologic findings were highly concordant within each study group,

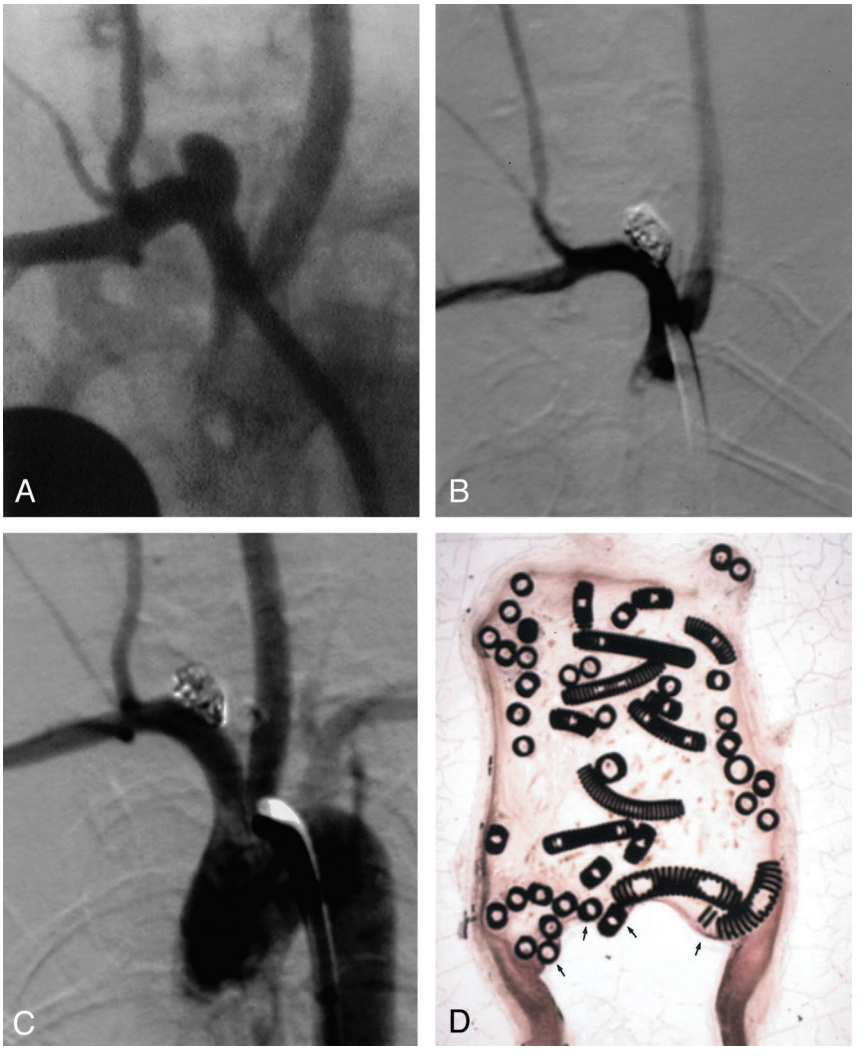

FIG 3. Subject 13, 12-week implantation.

A, DSA image obtained before embolization. The aneurysm is 3.6 × 3.9 × 4.1 mm (width × neck size × length).

B, DSA image obtained immediately after embolization depicts 100% occlusion.

C, DSA image obtained before euthanasia and 12 weeks after coil implantation shows no change.

D, Photomicrograph shows that the aneurysmal cavity is filled with coils and well-organized tissue, with no residual thrombus (hematoxylin-eosin stain, original magnification ×12.5). Minimal tissue thickness is present over the coils (*arrows*).

as long as 12 weeks after embolization. These findings indicate that aneurysmal domes remain nearly completely filled with unorganized blood for longer than 4 weeks after embolization. At 12 weeks after embolization, connective tissue replaced most of the blood products in the dome, but the exact type of tissue remains impossible to characterize with the embedding and staining techniques used in our study. Fibrin represents the predominant tissue overlying the aneurysmal neck at 2 weeks, and a thin layer of spindle cells becomes the predominant tissue at later time points. In all cases, however, at least some coils along the aneurysmal neck remained completely devoid of covering tissue; this finding suggests that the growth of spindle cells across the aneurysmal neck is stimulated and supported by the induced thrombus rather than the coils themselves. The origin of the spindle cells remains unknown; they may originate from the adjacent arterial wall or the circulating blood elements. In total, these angiographic and histologic findings add further evidence that the responses in the rabbit elastase-induced aneurysmal model closely mimics the response to coil embolization in humans.

Unlike the excellent concordance of histologic findings at time points as long as 12 weeks, the findings at 24 weeks were less clear. Unfortunately, one of four subjects was excluded for technical reasons. At 24 weeks, two subjects showed excellent healing, but histologic findings in one subject showed marked recanalization that was not evident at angiography. This subject had a neck width of nearly 5 mm, which was only slightly greater than the mean neck width for the entire study. However, this recanalized aneurysm had the widest neck in the 24-week study group; this observation suggests that longer follow-up might have shown coil compaction in some of the other study groups.

This study adds substantial information that is not available in previous reports of coil histologic features in the rabbit model of elastase-induced aneurysm (1, 7). First, the current study included angiographic correlation, which was absent in prior work. Second, the current study involved dense packing, as compared with loose packing in prior reports. Notably, histologic findings in the loosely packed and densely packed elastase aneurysms are relatively similar, with a predominance of unorganized thrombus at early time points and loose connective tissue present at later time points.

The findings presented herein concur with the angiographic and histologic findings of other investiga-

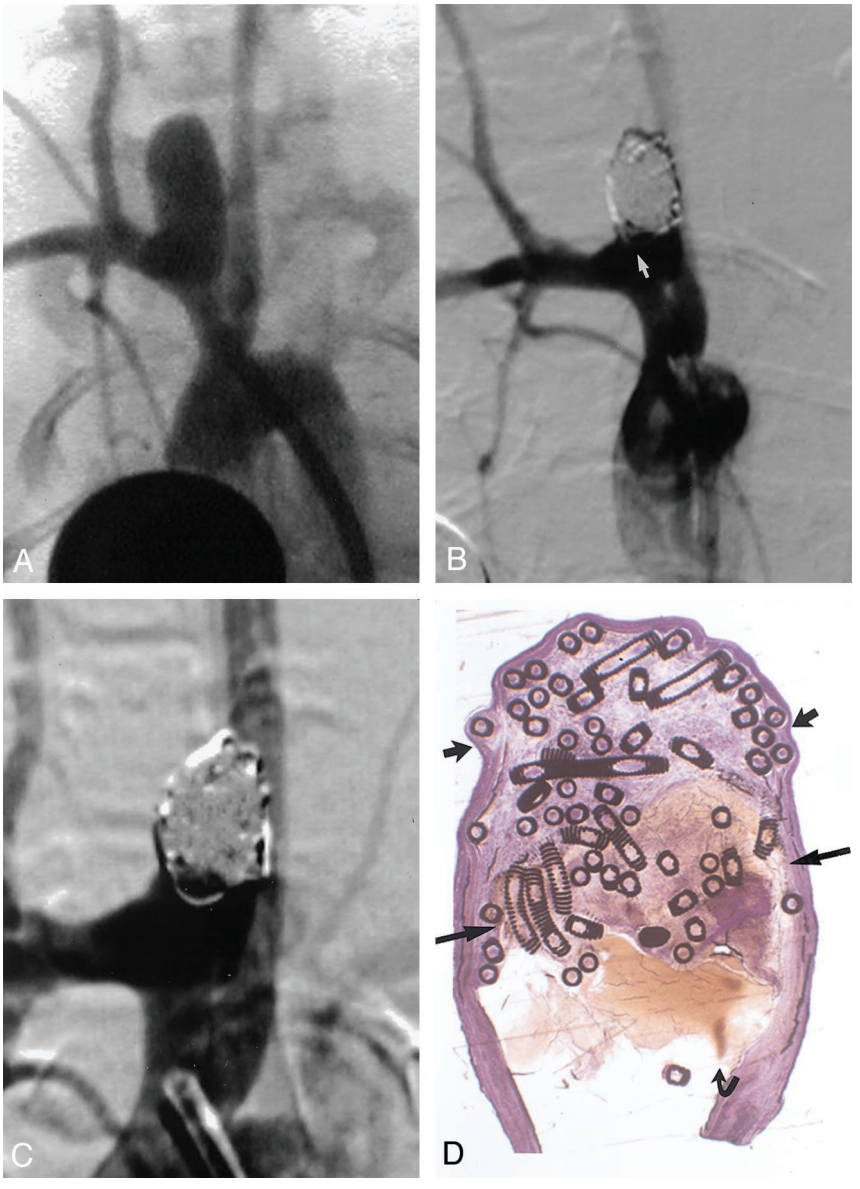

FIG 4. Subject 16, 24-week implantation.

A, DSA image obtained before embolization. The aneurysm is 5.4 × 4.9 × 12.2 mm (width × neck size × length).

B, DSA image obtained immediately after embolization depicts 90% occlusion with a single coil loop in the parent artery (*arrow*).

C, DSA image obtained before euthanasia and 6 months after coil implantation shows no change.

D, Three distinct regions were present at histologic analysis. The distal dome is filled with organized tissue (*short straight arrows*). The midportion of the dome demonstrates unorganized thrombus (*long straight arrows*). The neck region (*curved arrow*) shows persistent flow and probably coil compaction, which was difficult to identify at angiography (hematoxylin-eosin stain, original magnification ×8.3).

tors who used different types of experimental rabbit aneurysms. Using surgically created vein-patch aneurysms, Reul et al (10) and Spetzger et al (11) found that small areas of continued flow into the aneurysmal neck were apparent at histologic analysis but impossible to discern at angiography. As in our study, the growth of tissue over platinum coils was minimal, and complete occlusion was unusual, even with dense packing. The elastase-induced aneurysms used in the current study offer the advantage of ease of construction, with no need for microsurgical techniques; this advantage may allow wider dissemination of this technique, as compared with the vein-patch method.

The new coil system used in this study performed exceptionally well. Detachment difficulties occurred early in the study period and were essentially eradicated in later embolization sessions. The complex coils enabled embolization in even wide-necked aneurysms, as shown by the mean dome-to-neck ratio of 1:1. The challenging nature of these aneurysms, which have a low mean dome-to-neck ratio, is the likely explanation for the four cases in which coil loops protruded into the parent artery. Proper detachment occurred in most deployments, although these coils were made for research and development purposes, which accounted for some of the variability in the quality of the detachment mechanism.

This study has several limitations, which are primarily related to the small number of samples in each subgroup that precluded meaningful statistical comparisons. Furthermore, all studies of this type are limited by the lack of well-accepted grading schemes for both angiographic and histologic findings. Histologic evaluation was further hampered by the methacrylate embedding procedures, which preserve the morphology but make staining difficult. Finally, we estimated percentage of occlusion on the basis of angiographic findings, but these semiquantitative occlusion rates are difficult to quantify in exact terms. Various modifications of similar semiquantitative es-

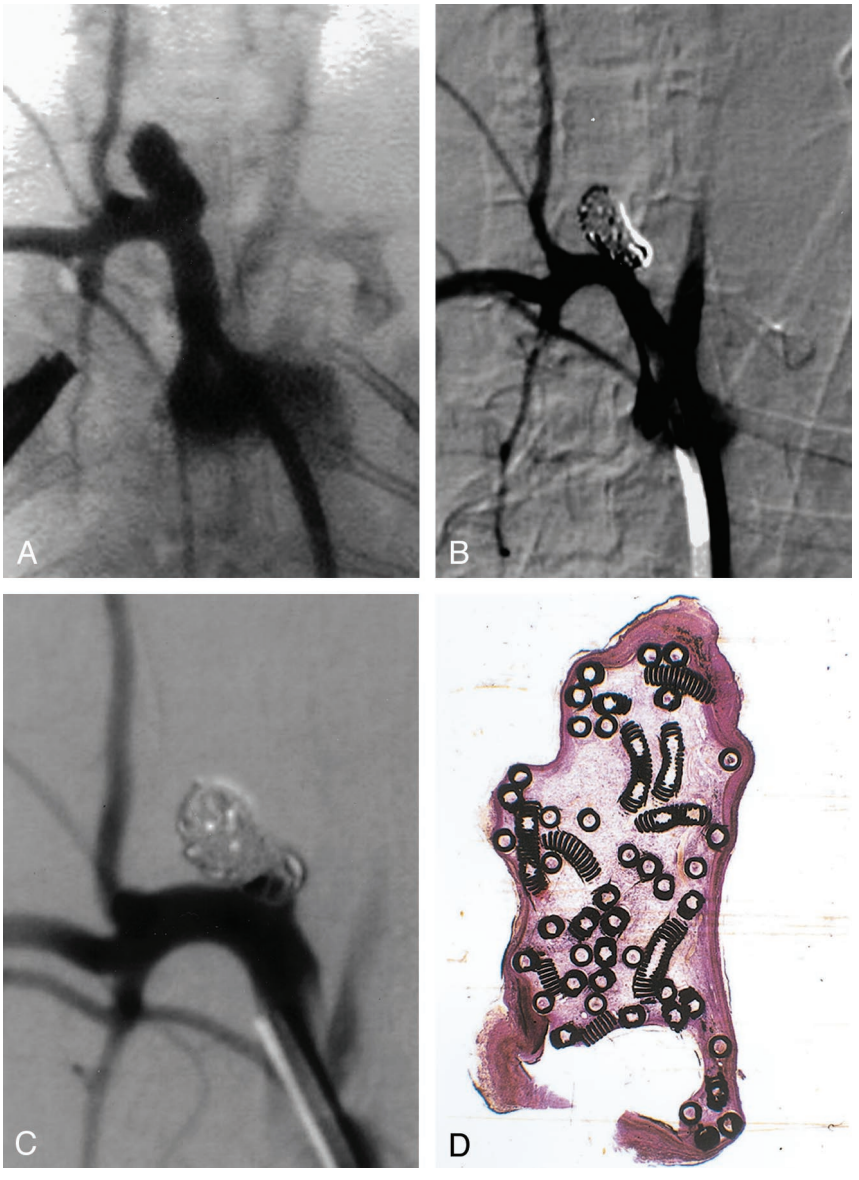

FIG 5. Subject 15, 24-week implantation.

A, DSA image obtained before embolization. The aneurysm is 4.1 × 4.5 × 6.5 mm (width × neck size × length).

B, DSA image obtained immediately after embolization depicts 95% occlusion.

C, DSA image obtained before euthanasia and 6 months after coil implantation demonstrates persistent flow at the aneurysmal neck but no change in the percentage occlusion.

D, The aneurysm is filled with organized tissue (hematoxylin-eosin stain, original magnification ×8.3).

timates are routinely used, as reported in the literature, but we acknowledge that the precise determination of occlusion rates remains difficult or impossible.

Conclusion

The new coil system evaluated in this study tracked, deployed, and detached in a predictable manner. Densely packed experimental aneurysms in rabbits demonstrate a reproducible histologic evolution that includes early fibrin coverage, delayed coverage by spindle cells, delayed resorption of intraaneurysmal thrombus, and occasional coil compaction.

References

1. Cloft HJ, Altes TA, Marx WF, et al. **Endovascular creation of an in vivo bifurcation aneurysm model in rabbits.** *Radiology* 1999;213:223–228
2. Geremia G, Haklin M, Brennecke L. **Embolization of experimentally created aneurysms with intravascular stent devices.** *AJNR Am J Neuroradiol* 1994;15:1223–1231
3. German W, Black S. **Experimental production of carotid aneurysms.** *N Engl J Med* 1954;3:463–468
4. Graves VB, Strother CM, Partington CR, Rappe A. **Flow dynamics of lateral carotid artery aneurysms and their effects on coils and balloons: an experimental study in dogs.** *AJNR Am J Neuroradiol* 1992;13:189–196
5. Graves VB, Strother CM, Rappe AH. **Treatment of experimental canine carotid aneurysms with platinum coils.** *AJNR Am J Neuroradiol* 1993;14:787–793
6. Kallmes DF, Altes TA, Vincent DA, Cloft HJ, Do HM, Jensen ME. **Experimental side-wall aneurysms: a natural history study.** *Neuroradiology* 1999;41:338–341
7. Kallmes DF, Helm GA, Hudson SB, et al. **Histologic evaluation of platinum coil embolization in an aneurysm model in rabbits.** *Radiology* 1999;213:217–222
8. Kerber CW, Buschman RW. **Experimental carotid aneurysms: I. Simple surgical production and radiographic evaluation.** *Invest Radiol* 1977;12:154–157
9. Mawad ME, Mawad JK, Cartwright JJ, Gokaslan Z. **Long-term histopathologic changes in canine aneurysms embolized with Guglielmi detachable coils.** *AJNR Am J Neuroradiol* 1995;16:7–13
10. Reul J, Weis J, Spetzger U, Konert T, Fricke C, Thron A. **Long-term angiographic and histopathologic findings in experimental aneurysms of the carotid bifurcation embolized with platinum and tungsten coils.** *AJNR Am J Neuroradiol* 1997;18:35–42
11. Spetzger U, Reul J, Weis J, Bertalanffy H, Thron A, Gilsbach JM.

Microsurgically produced bifurcation aneurysms in a rabbit model for endovascular coil embolization. *J Neurosurg* 1996;85:488–495
12. Stehbens WE. **Chronic vascular changes in the walls of experimental berry aneurysms of the aortic bifurcation in rabbits.** *Stroke* 1981;12:643–647
13. Wakhloo AK, Schellhammer F, de Vries J, Haberstroh J, Schumacher M. **Self-expanding and balloon-expandable stents in the treatment of carotid aneurysms: an experimental study in a canine model.** *AJNR Am J Neuroradiol* 1994;15:493–502
14. Fujiwara NH, Cloft HJ, Marx WF, Short JG, Jensen ME, Kallmes DF. **Serial angiography in an elastase-induced aneurysm model in rabbits: evidence for progressive aneurysm enlargement after creation.** *AJNR Am J Neuroradiol* 2001;22:698–703
15. Altes TA, Cloft HJ, Short JG, et al. **1999 ARRS Executive Council Award: Creation of saccular aneurysms in the rabbit: a model suitable for testing endovascular devices—American Roentgen Ray Society.** *AJR Am J Roentgenol* 2000;174:349–354
16. Cognard C, Weill A, Spelle L, et al. **Long-term angiographic follow-up of 169 intracranial berry aneurysms occluded with detachable coils.** *Radiology* 1999;212:348–356